Infection-Derived Monocytic MDSCs Require TGF-β to Suppress Filarial-Specific IFN-γ But Not IL-13 Release by Filarial-Specific CD4+ T Cells *In Vitro*

Ruth S. E. Tamadaho[1], Manuel Ritter[1], Anna Wiszniewsky[1], Kathrin Arndts[1], Matthias Mack[2], Achim Hoerauf[1,3] and Laura E. Layland[1,3]*

[1] Institute of Medical Microbiology, Immunology and Parasitology (IMMIP), University Hospital Bonn (UKB), Bonn, Germany, [2] Department of Nephrology, University Hospital Regensburg, Regensburg, Germany, [3] German Centre for Infection Research (DZIF), Partner Site, Bonn-Cologne, Bonn, Germany

Lymphatic filariasis (LF) remains a major health problem with severe economic repercussions in endemic communities of Sub-saharan Africa, South-East Asia and South America. The rodent-specific nematode *Litomosoides sigmodontis* (Ls) is used to study the immunomodulatory potential of filariae and research has elucidated pathways involving regulatory T cells (Tregs), IL-10 producing cells and alternatively activated macrophages (AAMs) and that CD4+ T cells play a paramount role during infection. Myeloid-derived suppressor cells (MDSCs) have been identified and characterised in man in cancer and other pathologies. The hallmark of MDSC populations is the suppression of T and B cell responses using various mechanisms, which are mostly specific to the pathology or setting. However, until now, it remains unclear whether they play a role in filarial-specific responses. We report here that monocytic MDSCs (Mo-MDSCs, CD11b+Ly6C+Ly6G-) and polymorphonuclear MDSCs (PMN-MDSCs, CD11b+Ly6Cint/loLy6G+) expanded in the thoracic cavity (TC, the site of infection) and correlated positively with filarial life-stages in Ls-infected BALB/c mice. *In vitro*, only infection-derived Mo-MDSCs showed a suppressive nature by preventing IL-13 and IFN-γ secretion from filarial-specific CD4+ T cells upon co-culture with soluble worm extract. This suppression was not mediated by IL-10, IL-6 or TNF-α, and did not require cell-contact, nitric oxide (NO), IL-4/IL-5 signalling pathways or CCR2. Interestingly, neutralizing TGF-β significantly rescued IFN-γ but not IL-13 production by filarial-specific CD4+ T cells. In comparison to naive cells, PCR array data showed an overall down-regulation of inflammatory pathways in both infection-derived Mo-MDSCs and PMN-MDSCs. In conclusion, these primary data sets show activity and expansion of MDSCs during Ls infection adding this regulatory cell type to the complex milieu of host responses during chronic helminth infections.

Keywords: *Litomosoides sigmodontis*, MDSCs, cytokines, microfilariae, immune-regulation, TGF-β

INTRODUCTION

Approximately, 65 million people are infected with LF worldwide (1). To understand mechanisms underlying immunity to filarial infections in man, such as *Wuchereria bancrofti* which elicits lymphatic filariasis (LF) (2, 3), researchers employ the *Litomosoides sigmodontis* (*L. sigmodontis*, Ls) rodent model since it reflects several aspects of LF infection. This includes partial patency since only a portion of immunocompetent BALB/c mice become patent (release microfilariae (MF) into the periphery) when naturally infected with Ls (4–6). The development of adult worms from larval stages in the host provokes different immune reactions and encompasses both innate (neutrophils, eosinophils and basophils) and adaptive responses (T and B cells). Indeed, both filarial-specific CD4$^+$ T cells and Th2 responses have been found to be essential for Ls development and host immunity (6–8). Moreover, lack of Th2 associated cytokines, such as IL-4, IL-13 and IL-5, disables the effects of neutrophils and eosinophils on controlling worm burden and leads to elevated MF loads (9–11). Interestingly, studies have also shown that IFN-γ supports neutrophil-mediated clearance of Ls adult worms and suggested that Th1 and Th2 immune responses act in a synergistic manner in order to control Ls infection (12, 13). Furthermore, infection with Ls induces regulatory cell populations including Tregs, IL-10 producing cells and alternatively activated macrophages (AAMs) that can affect CD4$^+$ T cells by making them hyporesponsive to the nematode (6, 14–17). In this study, we investigated the yet unexplored role of another regulatory cell population: Myeloid-Derived Suppressor Cells (MDSCs). Two subsets of MDSCs, the monocytic MDSCs (Mo-MDSCs, CD11b$^+$Ly6C$^+$Ly6G$^-$) and the polymorphonuclear MDSCs (PMN-MDSCs, CD11b$^+$Ly6C$^{int/lo}$Ly6G$^+$) have been identified in patients and murine models of disease. These include cancer, systemic inflammation and sepsis, autoimmune diseases as well as bacterial, viral and parasitic infections (18–26). Mo-MDSCs and PMN-MDSCs are reported to suppress T and B cell responses through receptors, cytokines, or soluble factors as reviewed (20, 27). It has been shown that in infections caused by *Heligmosomoides polygyrus bakeri*, isolated CD11c$^-$CD11b$^+$Gr1$^+$ cells, likely MDSCs, suppressed OVA-specific CD4$^+$ T cell proliferation in a nitric oxide (NO)-dependent manner and nematode-specific IL-4 responses *in vitro*. Also, an adoptive transfer of these cells induced higher parasite burden indicating that these cells promoted chronic infection (28). This current work explored the role of Mo- and PMN-MDSCs over the course of Ls infection in BALB/c mice. Interestingly, both MDSC subsets were present in the thoracic cavity (TC), the site of infection and levels

positively correlated with worm load. Since cells were virtually absent in naive mice, this indicates that MDSCs are part of the immune repertoire that is specifically drawn to the TC during infection. To test functional responses of infection-derived MDSCs subsets, we designed an *in vitro* MDSC:T cell co-culture assay and revealed that Mo-MDSCs but not PMN-MDSCs showed high suppressive abilities on the production of IL-13 and IFN-γ but not IL-5 by Ls-specific CD4$^+$ T cells. This suppression was independent of cell-contact, nitric oxide, IL-10, IL-6, TNF-α and the receptors CCR2 and IL-4Rα. Further analyses demonstrated that Mo-MDSCs used the TGF-β pathway to impair the production of IFN-γ but not IL-13. Collectively, this study reveals that the expansion of MDSCs subsets during Ls infection is a specific host response and Mo-MDSCs have a defined role in controlling Ls-specific IL-13 and IFN-γ production from CD4$^+$ T cells.

MATERIAL AND METHODS

Ethics Statement

Wildtype (WT) and IL-4Rα/IL-5dKO BALB/c mice were kept under specific-pathogen-free (SPF) conditions at the Institute of Medical Microbiology, Immunology and Parasitology (IMMIP), University Hospital of Bonn (UKB), Bonn, Germany. Animals were bred in accordance with German animal protection laws and the EU guidelines 2010/63/E4. All *in vivo* experiments were reviewed and approved by the appropriate committee (Landesamt für Natur, Umwelt und Verbraucherschutz, NRW, Germany).

Animal Maintenance and Infections With *L. sigmodontis*

WT BALB/c mice were obtained from Janvier Labs (Le Genest-Saint-Isle, France). IL-4Rα/IL-5 dKO BALB/c mice were originally provided by Prof. Dr. Klaus Matthaei, Australia National University College of Medicine, Biology and Environment, Canberra, Australia. Natural infections with Ls were performed as previously described (6, 9, 10, 29). Endotoxin-free LsAg extracts were prepared from adult Ls worms and stored at -80°C until required (6, 9, 29).

Parasite Recovery and Determination of MF Load

Worms were recovered from the TC of individually infected BALB/c female mice between day 70-72 post-infection (p.i.) as previously described and gender and numbers were determined microscopically (6, 8, 30). To determine MF load, 50 μl of blood or TC fluid from individually infected mice were placed in 300 μl Hinkelmann solution. After incubation at room temperature (RT) for 20-30 min, the suspension was centrifuged (Multifuge 4KR, Heraeus Holding GmbH, Hanau, Germany) at 1800 rpm for 5 minutes and the supernatant (SN) was discarded. MF were counted in the pellet using a microscope (Leica Microsystems GmbH, Wetzlar, Germany).

Abbreviations: BMDC, bone-marrow derived dendritic cells; GM-CSF, granulocyte macrophage colony stimulating factor; L-NMMA, monomethyl-L-arginine monoacetate salt; *L. sigmodontis, Litomosoides sigmodontis;* LsAg, *L. sigmodontis* worm antigen preparation; MDSCs, myeloid-derived suppressor cells; mLN, mediastinal lymph nodes; MF, microfilariae; Mo-MDSCs, monocytic MDSCs; NO, nitric oxide; NOS, nitric oxide synthase; PMN-MDSCs, polymorphonuclear MDSCs; ROS, reactive oxygen species; TC, thoracic cavity.

BMDC Preparation

Following erythrocyte-depletion of RBCs from leg bones (hip to ankle) of WT BALB/c mice, GM-CSF (20 ng/mL, Peprotech, New Jersey, USA) derived dendritic cells were generated over 7 days using the previously described protocol (6).

CD4$^+$ T Cell Isolation

An enriched T cell fraction from pooled spleen and mediastinal lymph nodes (mLN) between 70-72 days Ls-infected BALB/c mice were obtained after depletion of antigen presenting cells (APCs) using MHC class II beads and MACS technology (Miltenyi Biotech, Bergisch Gladbach, Germany). Resulting cells were then stained with anti-CD4 (clone RM4-5) APC-conjugated and anti-CD25 (clone PC61.5) PE-conjugated antibodies (Thermo Fisher Scientific). CD4$^+$CD25^{neg} and CD4$^+$CD25^{hi} T cells were then isolated using the FACS DIVA cell sorter (BD Biosciences, Heidelberg, Germany). We purposely removed the CD4$^+$CD25^{hi} T cells from the main CD4$^+$ T cell population based on the findings from our earlier studies (6, 31, 32) since this now removed potential regulatory T cells (CD4$^+$CD25^{hi}Foxp3$^+$) from the co-cultures allowing a more accurate assessment of the MDSC suppressive ability on effector CD4$^+$ T cells fractions. Cells were isolated using BD FACS Aria III Cell Sorter (BD Biosciences, Heidelberg, Germany) at the Flow Cytometry Core Facility (FCCF), Bonn.

MDSC Isolation

Mo-MDSCs and PMN-MDSCs were isolated from the TC of infected BALB/c mice *via* sorting. After blocking (anti-CD16/CD32, clone 93) (Thermo Fisher Scientific) and staining cells with anti-CD11b (clone M1/70) Alexa Fluor 488-, anti-CD45 (clone 30-F11) PerCP Cy5.5-, anti-Ly6C (clone HK1.4) APC Cy7- and anti-Ly6G (clone 1A8) PE-conjugated antibodies (all from Biolegend, Koblenz, Germany) MDSC populations were identified using the gating strategy depicted in **Figure 1A** adapted from (33). Cells were isolated using BD FACS Aria III Cell Sorter (BD Biosciences, Heidelberg, Germany) at the Flow Cytometry Core Facility (FCCF), Bonn. A purity rate of 94% and 100% was obtained after re-acquiring and analysis of Mo-MDSCs and PMN-MDSCs, respectively (**Figure S1A**). To determine the viability of the isolated cells, TC cells of infected BALB/c mice were stained with anti-CD11b (clone M1/70) BV510-, anti-CD45 (clone 30-F11) AF700-, anti-Ly6C (clone HK1.4) APC Cy7-, anti-Ly6G (clone 1A8) PE-conjugated antibodies and propidium iodide (PI) (all from Biolegend, Koblenz, Germany) (**Figure S1B**). At least 87% of isolated cells were alive prior to co-culture (**Table S1**).

In Vitro Filarial-Specific MDSC:T Cell Co-Culture Assays

To perform the standard MDSC:T cell co-culture assay, 1×10^5 CD4$^+$ T cells from WT Ls-infected BALB/c mice (between days 70-72 p.i.) were co-cultured with 5×10^4 GM-CSF-derived BMDC from naive WT BALB/c mice in the presence or absence of Ls-derived 1×10^5 Mo- or PMN- MDSCs and stimulated with 50 µg/mL Ls antigen (LsAg) in 96-well plates (37°C, 5% CO_2). In some assays MDSCs

were derived from IL-4Rα/IL-5 dKO BALB/c mice. After 24 or 72 hours, supernatants were collected and analysed for cytokine levels. In some assays, neutralizing antibodies: anti-CCR2 (20 µg/mL), anti-IL-10 (2 µg/mL), anti-IL-6 (10 µg/mL) anti-TGF-β (10 µg/mL), anti-TNF-α (0.5 µg/mL) or inhibitors (L-NMMA, 5 µM, at 0 hours or 0, 24 and 48 hours) and their isotype controls (mAb mouse IgG1 isotype control, clone MOPC-21 from BioXcell for anti-TGF-β and mAb rat IgG2B isotype control, clone 141945 from R&D systems for anti-CCR2) were added at least 30 minutes before Ls stimulation. Furthermore, the effect of the co-culture set-up on MDSC function was assessed. For this, LsAg was added to the co-culture after 60 minutes. Anti-CCR2 (clone MC-21) antibody was a kind gift from Prof. Dr. Matthias Mack (University Hospital Regensburg); anti-TGF-β (clone 1D11.16.8) was purchased from BioXcell, West Lebanon, USA; anti-IL-10 (clone JES052A5), anti-IL-6 (clone MP520F3) and anti-TNF-α (clone MP6-XT22) from R&D systems, Wiesbaden-Nordenstadt, Germany and L-NMMA was obtained from Abcam, Cambridge, UK. In transwell experiments, culture conditions remained the same except that MDSC subsets were cultured in an insert (0.4 µM pore size; Corning GmbH Life Sciences, Wiesbaden, Germany), permeable to soluble factors but not allowing physical cell-contact (34, 35).

Cytokine Determination

Cytokine concentrations in the culture supernatants of re-stimulation assays were determined by ELISA according to the manufacturer's instructions (IFN-γ and IL-13 Thermo Fisher Scientific; IL-5 BD Biosciences). ELISA plates were read and analysed at 450 and 570 nm using a Spectra Max 340pc384 photometer and SOFTmax Pro 3.0 software (Molecular Devices, Sunnyvale, California, USA).

Flow Cytometry Staining of MDSCs

Frequencies of MDSC subsets in Ls-infected BALB/c mice were determined using cells collected from the TC. After blocking (anti-CD16/CD32, clone 93) (Thermo Fisher Scientific), cells were stained with the antibodies used for MDSC isolation (section 3.6 MDSC isolation). Expression levels were determined using the FACS Canto flow cytometer (BD Biosciences) and analysis was performed using the gating strategy shown in **Figure 1A**, adapted from (33) with FlowJo VX software (Tree Star, Inc, Ashland, Oregon, USA).

Gene Expression Analysis

In order to evaluate the differences in the expression of 84 genes between isolated Mo- and PMN-MDSC populations (see *MDSC Isolation*) from pooled Ls-infected BALB/c mice (n=10), PCR Arrays using the RT2 SYBR Green Mastermix kit (Qiagen, Hilden, Germany) and the RT2 Profiler PCR Array Mouse Innate and Adaptive Immune Responses kit (Qiagen) were performed. These two subsets of MDSCs were also isolated from naive mice to serve as controls (n=30). 20 µl PCR components mix were added to each well of the RT2 Profiler PCR Array using Qiagility device (Qiagen), followed by cycling using a Rotor Gene Q (Qiagen). Data were analysed using the online RT2 Profiler PCR Array Data analysis 3.5 software at the
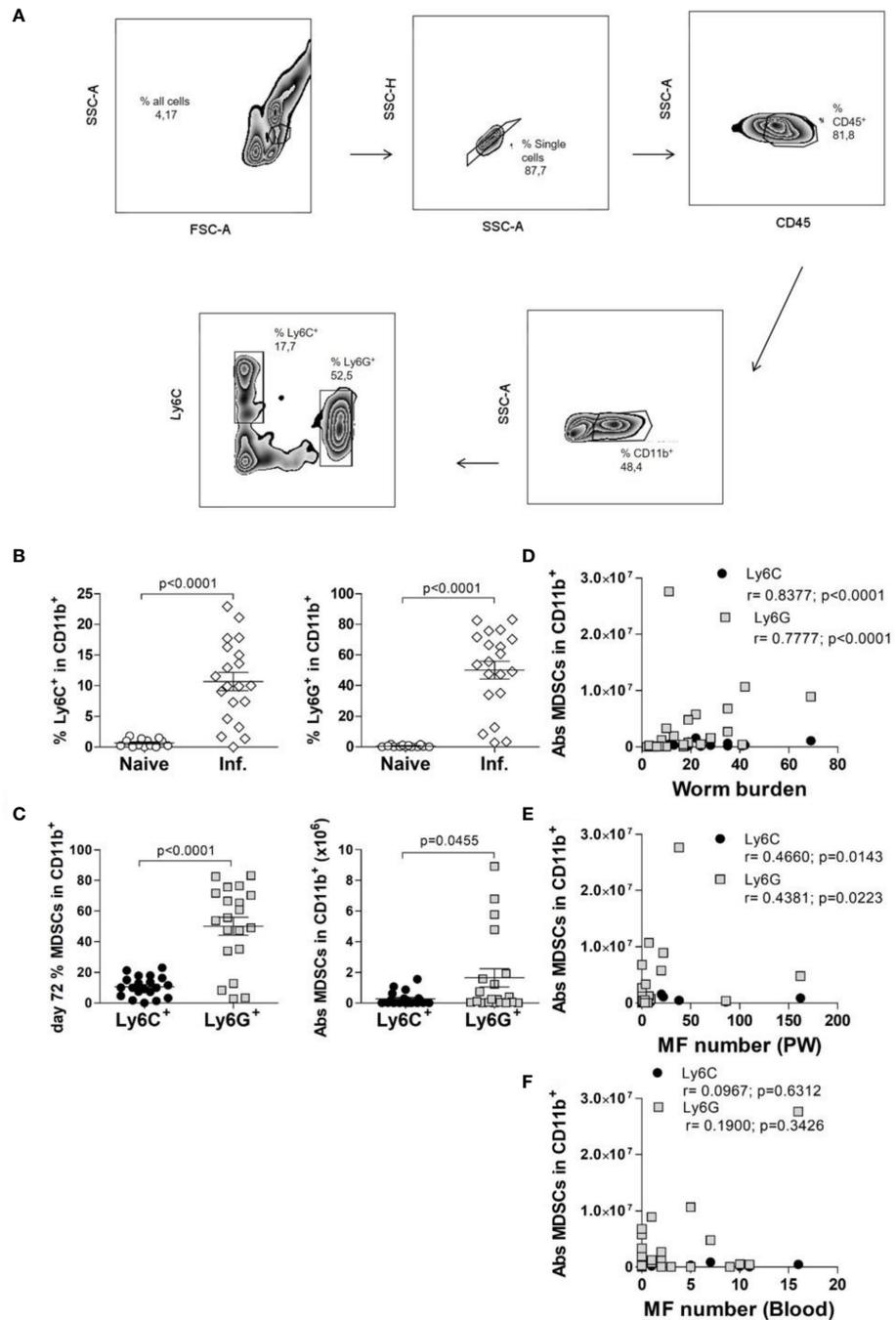
FIGURE 1 | MDSC subsets accumulate at the site of infection following exposure to *Litomosoides sigmodontis*. **(A)** Monocytic (CD11b$^+$Ly6C$^+$Ly6G$^-$, Mo-MDSCs or Ly6C$^+$) and polymorphonuclear (CD11b$^+$Ly6C$^{int/lo}$Ly6G$^+$, PMN-MDSCs or Ly6G$^+$) MDSC populations were discriminated by gating on single CD45$^+$ cells that co-expressed CD11b. Further discrimination of CD45$^+$CD11b$^+$ cells using Ly6C and Ly6G markers revealed Mo-MDSCs and PMN-MDSCs respectively. **(B)** Percentage of Mo-MDSCs and PMN-MDSCs within the CD11b$^+$ population in naive and day 72 Ls-infected mice (Inf.). Symbols show individual values of n=13 naive and n=20 Ls-infected mice from two independent infection studies. Statistical significances between the indicated groups were obtained after a Mann-Whitney test. **(C)** Comparison of MDSC subsets within the CD11b$^+$ compartment on day 72 p.i. of Ls-infected mice as percentage or absolute (Abs) cell number. Symbols show values from individual mice (n=20) from two independent infection studies. Statistical analysis was performed using the Mann-Whitney test. Correlation of numbers of both MDSC subsets with the worm load **(D)** and MF numbers in the TC **(E)** and in blood **(F)**. Data are from infected mice (n=27) pooled from three independent infection studies. Statistical significances were tested using the Spearman correlation test.

sabiociences.com website (Qiagen) and gene expression was normalized to Beta-actin. The threshold cycle (Ct) cut-off was set to 33 and the fold-change varied between 0.0001 and 15789. Fold-change values greater than one indicate a positive- or an up-regulation, and fold-change values less than one indicate a negative or down-regulation.

Statistical Analysis

Statistical analyses were performed using SPSS (IBM SPSS Statistics 25, Armonk, NY, USA) and graphs were generated using the software PRISM 5.02 (GraphPad Software, Inc., La Jolla, USA). After column statistics (D'Agostino & Pearson normality test, Shapiro-Wilk normality test and Kolmogorov Smirnov normality test), statistical differences between three or more groups were observed using ANOVA with Tukey posthoc test, for a parametric distribution. If data were non-parametric, a Kruskal-Wallis with Dunn's posthoc test was used. For correlation analysis, statistical significances were tested using the Spearman correlation test. P-values of 0.05 or less were considered significant.

RESULTS

MDSC Populations Expand During *Litomosoides sigmodontis* Infection

Commonly, MDSCs are classified as monocytic (Mo-MDSCs = Ly6C, CD11b$^+$Ly6C$^+$Ly6G$^-$, labelled as Ly6C$^+$) or polymorphonuclear (PMN-MDSCs = Ly6G, CD11b$^+$Ly6C$^{int/lo}$Ly6G$^+$, labelled as Ly6G$^+$) [18, 19]. Earlier studies revealed that following infection with Ls in BALB/c mice, the peak of MF (reflecting the transmission life-stage) was between day 70-72 p.i [6]. To determine whether frequencies of MDSC populations are altered during Ls infection, cells were monitored at the site of infection (TC) and subsets were distinguished from one another *via* flow cytometry using the scheme depicted in **Figure 1A**.

Very few Mo-MDSCs or PMN-MDSCs were present in the TC of naïve mice (**Figure 1B**) whereas substantial numbers of these cells comprised the cellular milieu in Ls-infected mice 72 days p.i. (**Figure 1B**). Moreover, frequencies and cell numbers of PMN-MDSCs were significantly higher than Mo-MDSCs (**Figure 1C**). Correlation analysis of worm burden or MF counts with MDSC numbers also indicated that levels of both Mo-MDSCs and PMN-MDSCs positively correlated with worm burden (**Figure 1D**) and MF in the TC (**Figure 1E**). However, no correlation was displayed between MDSC levels in the TC and released MF numbers in blood (**Figure 1F**). These data show that Mo-MDSCs and PMN-MDSCs infiltrate the TC of Ls-infected mice and positively correlate with parasite load at the site of infection.
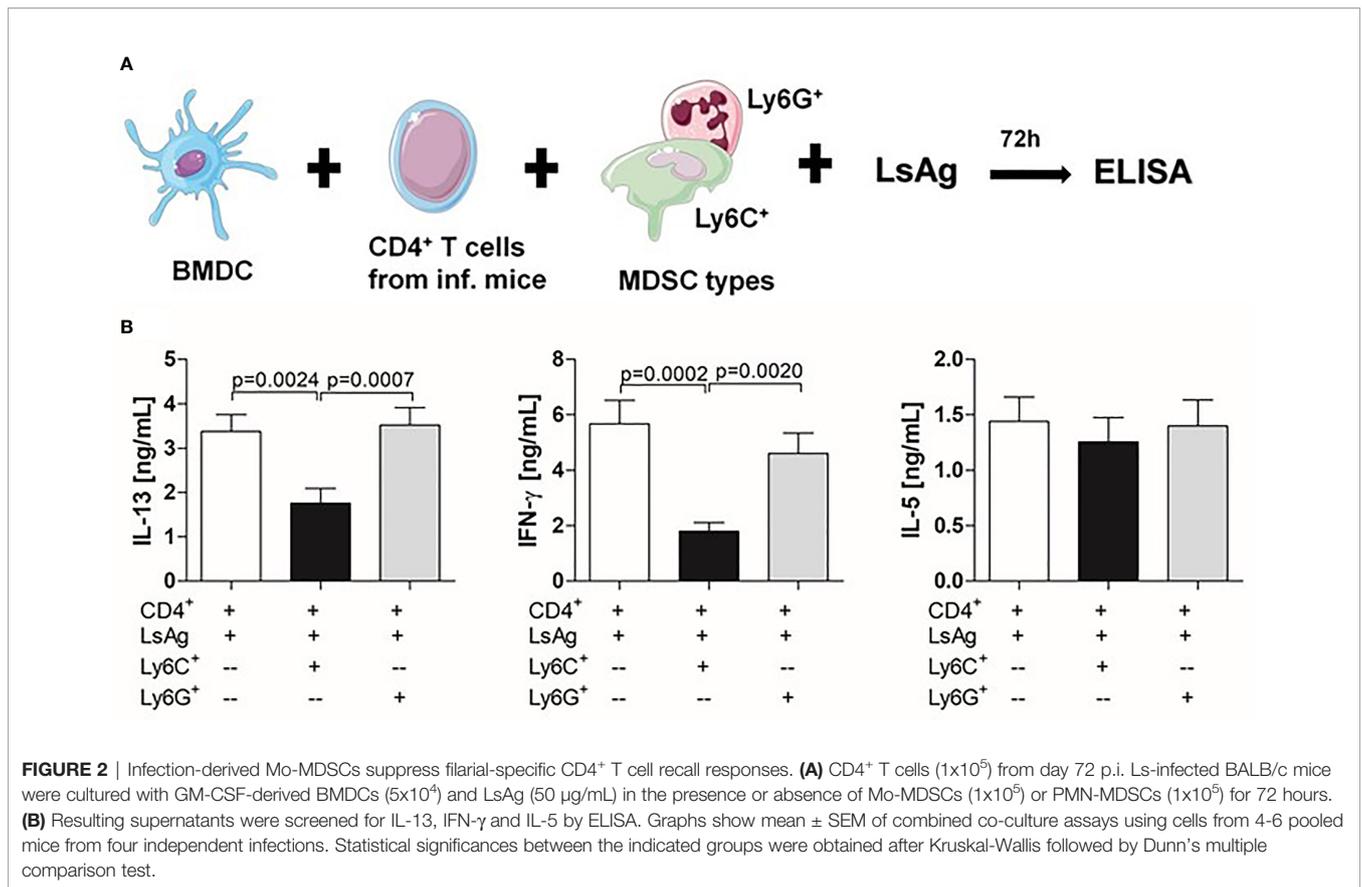
Mo-MDSCs But Not PMN-MDSCs Suppress Ls-Specific CD4$^+$ T Cell Responses

To test the suppressive properties of Mo-MDSCs and PMN-MDSCs that arose during Ls infection, an *in vitro* MDSC:T cell

co-culture assay was designed (**Figure 2A**). Earlier studies have shown that CD4$^+$ T cells from Ls-infected but not naïve BALB/c mice can be re-stimulated *ex vivo* with LsAg (a soluble extract prepared from adult Ls worms) [6] (**Figure S2A**). Thus, CD4$^+$ T cells (without the Treg compartment) from Ls-infected WT BALB/c mice (70-72 days p.i.) were co-cultured with GM-CSF-derived BMDC from WT BALB/c naïve mice and stimulated with LsAg in the presence or absence of Mo- or PMN- MDSCs from Ls-infected mice in a 1:1 ratio (MDSCs:T cells). This assay revealed that Mo-MDSCs were able to significantly suppress the production of IL-13 and IFN-γ but not IL-5 by filarial-specific CD4$^+$ T cells (**Figure 2B** *c.f.* white and black bars). Surprisingly, PMN-MDSCs were not able to suppress the production of any of those measured cytokines (**Figure 2B** *c.f.* white and grey bars). Of note, when compared to the main read-out parameter DC+CD4$^+$+LsAg, other controls had negligible levels of IL-13 and IFN-γ (**Figure S2B**) when stimulated with LsAg. Similarly, co-culture of Mo-MDSCs with GM-CSF-derived DC (without CD4$^+$ T cells) had very low cytokine levels (**Figure S3**) Moreover, the observed suppression shown by Mo-MDSCs was not caused by cell death (or whether antigen stimulation occurred before or after Mo-MDSCs were added to co-culture), since discrimination of dying (or adding Mo-MDSCs after antigen stimulation) still resulted in suppression of IL-13 and IFN-γ (**Figures S1B, C**). To determine whether the suppressive ability of Mo-MDSCs was connected to the infection state of the mouse (patent or latent), further assays were performed using Mo-MDSCs isolated from either MF+ or MF- mice. **Figure S4** shows that the suppressive capacity of Mo-MDSCs on the production of IL-13 (**Figure S4A**) or IFN-γ (**Figure S4B**) by Ls-specific CD4$^+$ T cells is independent on the infection state of the mouse.

Receptor-Dependent Pathways Are Not Crucial for Mo-MDSC Function

Research has indicated that MDSCs suppress T cell responses through the IL-4Rα. For example, cancer patients have been shown to have higher levels of MDSCs expressing IL-4Rα [36, 37]. Moreover, studies have reported that suppression through IL-4Rα is only attributed to the Mo-MDSC subset [38]. Therefore, in order to decipher the mechanism(s) by which Mo-MDSCs suppress Ls-specific CD4$^+$ T cell responses, we investigated the outcome of the suppressive ability of infection-derived Mo-MDSCs from IL-4Rα/IL-5 dKO BALB/c mice since earlier studies showed that these mice present high worm burden and MF load in the absence of these Th2 cytokines [9, 11]. Surprisingly, Mo-MDSCs derived from Ls-infected IL-4Rα/IL-5 dKO BALB/c mice were able to suppress IL-13 and IFN-γ production by Ls-specific CD4$^+$ T cell responses in a similar manner to those derived from WT BALB/c (**Figures 3A, B**). This indicates that neither the IL-4Rα nor IL-5 was involved in the observed suppression. In regards to MDSC numbers in the TC, levels of Mo-MDSCs in either percentage or absolute cell number were significantly higher in Ls-infected IL-4Rα/IL-5 dKO BALB/c (**Figures S5A, C**) when compared to those in WT mice whereas populations of PMN-MDSCs remained comparable (**Figures S5B, D**). There was no difference in MDSC amounts in naïve

FIGURE 2 | Infection-derived Mo-MDSCs suppress filarial-specific CD4$^+$ T cell recall responses. **(A)** CD4$^+$ T cells (1x10^5) from day 72 p.i. Ls-infected BALB/c mice were cultured with GM-CSF-derived BMDCs (5x10^4) and LsAg (50 μg/mL) in the presence or absence of Mo-MDSCs (1x10^5) or PMN-MDSCs (1x10^5) for 72 hours. **(B)** Resulting supernatants were screened for IL-13, IFN-γ and IL-5 by ELISA. Graphs show mean ± SEM of combined co-culture assays using cells from 4-6 pooled mice from four independent infections. Statistical significances between the indicated groups were obtained after Kruskal-Wallis followed by Dunn's multiple comparison test.

IL-4Rα/IL-5 dKO BALB/c when compared WT mice (3.103% ± 0.345 vs 3.66% ± 1.149, respectively). CCR2 is a receptor present on the surface of Mo-MDSCs but not PMN-MDSCs (39) and reports have suggested that this receptor influences the suppressive activity of Mo-MDSCs (40–42). However, in assays blocking the CCR2 receptor, Mo-MDSCs were still capable of suppressing IL-13 and IFN-γ production by Ls-specific CD4$^+$ T cells, (**Figures 3C, D** and **S6A, B** for data including isotype controls).
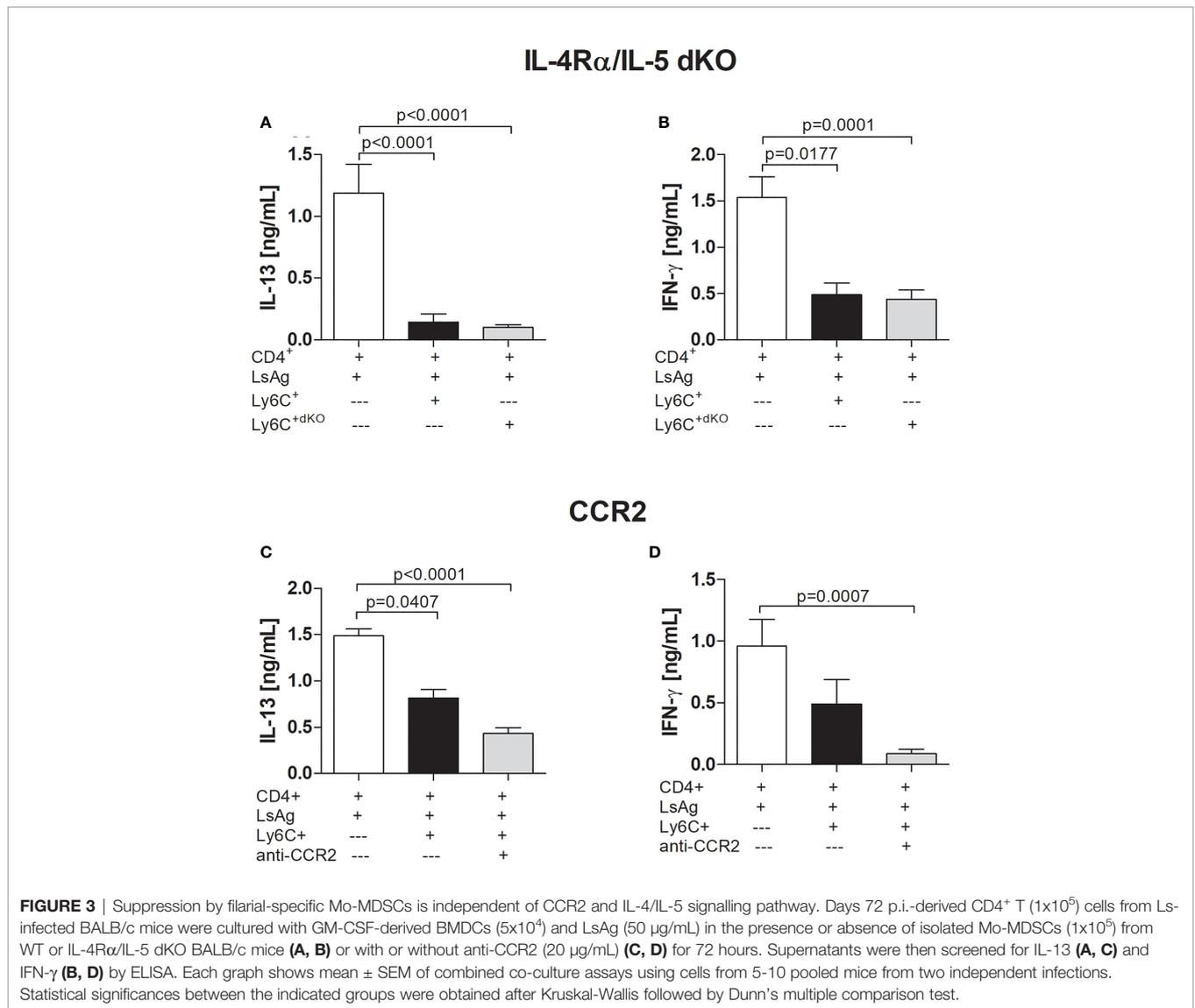
Next, we assessed the requirement of cell-contact for Mo-MDSCs to suppress IL-13 and IFN-γ production by filarial-specific CD4$^+$ T cells using a transwell assay (**Figures S7A, B**). To avoid cell-contact, Mo-MDSCs were placed in an insert. Again, suppression of T cell cytokine production remained unaltered between MDSC co-cultures with or without the insert indicating that cell-contact was not required. These data tallied with the findings on the IL-4Rα receptor and emphasised that suppression was not receptor mediated.

MDSC-Related Cytokines and Nitric Oxide Pathways Are Not Essential for Mo-MDSC Suppression of LsAg-Specific CD4$^+$ T Cell Responses

Evidence has been provided that MDSCs function through either soluble factors (43, 44) or receptors (41, 45) and since we found that suppression of CD4$^+$ T cell responses by infection-derived

Mo-MDSCs was not cell-contact dependent, we explored the requirement of cytokines using neutralizing antibodies. Increased levels of IL-10 and IL-6 levels have been associated with the augmentation of Mo-MDSC levels in patients or models of cancer and other diseases (46–49). Additionally, studies have demonstrated that TNFR2 expression is required for the generation and function of Mo-MDSCs (45, 50, 51). Here, we found that the Mo-MDSC-mediated suppression of IL-13 (**Figures 4A-C**) or IFN-γ (**Figures 4D-F**) by Ls-specific CD4$^+$ T cells was sustained after neutralizing IL-10 (**Figures 4A, D**), IL-6 (**Figures 4B, E**) or TNF-α (**Figures 4C, F**), indicating that these cytokines were not relevant for Mo-MDSC suppressive activity.

NO and ROS are factors associated with MDSC function and a study has reported that Mo-MDSCs limited autologous B cell proliferation and antibody production in a NO and PGE$_2$-dependent manner (43, 52) and recent findings showed that tumor-derived MDSCs regulated NO production in asthma pathogenesis (53). Interestingly, using a single application of L-NMMA (an inhibitor of nitric oxide synthase (NOS), an enzyme which catalyses NO production), we observed a trend of suppression of IFN-γ production by Ls-specific CD4$^+$ T cells in presence of Mo-MDSCs 24 hours after stimulation (**Figures 5A, B**). Upon 72 hours stimulation, both IL-13 and IFN-γ production were dampened by Mo-MDSCs and this was not affected by blocking NO pathways (**Figures 5C, D**). Moreover, this did not alter when multiple doses (at 0, 24 and

FIGURE 3 | Suppression by filarial-specific Mo-MDSCs is independent of CCR2 and IL-4/IL-5 signalling pathway. Days 72 p.i.-derived CD4$^+$ T (1x10^5) cells from Ls-infected BALB/c mice were cultured with GM-CSF-derived BMDCs (5x10^4) and LsAg (50 µg/mL) in the presence or absence of isolated Mo-MDSCs (1x10^5) from WT or IL-4Rα/IL-5 dKO BALB/c mice **(A, B)** or with or without anti-CCR2 (20 µg/mL) **(C, D)** for 72 hours. Supernatants were then screened for IL-13 **(A, C)** and IFN-γ **(B, D)** by ELISA. Each graph shows mean ± SEM of combined co-culture assays using cells from 5-10 pooled mice from two independent infections. Statistical significances between the indicated groups were obtained after Kruskal-Wallis followed by Dunn's multiple comparison test.

48 hours) of the inhibitor were added (**Figures 5E, F**). This suggests that Mo-MDSCs do not use NO pathways to suppress filarial-specific IL-13 and IFN-γ production by Ls-specific CD4$^+$ T cells.

TGF-β Is Critical for Filarial-Specific Mo-MDSC Suppression of IFN-γ

TGF-β is a cytokine which is usually associated with regulatory networks (54). Therefore, MDSC suppression assays were performed whilst blocking TGF-β. Interestingly, the presence of anti-TGF-β neutralizing antibody in the culture did not impair the ability of Mo-MDSCs to suppress IL-13 production (**Figures 6A** and **S6C**) but the suppression of IFN-γ production by filarial-specific CD4$^+$ T cells was significantly abrogated (**Figures 6B** and **S6D**). When compared to the main read-out parameter the secretion of TGF-β is diminished in the presence of Mo-MDSCs (**Figure S6E**, *c.f.* white and bars). Collectively, these data show that TGF-β is essential for the suppression of

IFN-γ production by filarial-specific CD4$^+$ T cells. **Figure 7** displays schematically the role of TGF-β in the suppression of IFN-γ production by filarial-specific CD4$^+$ T cells.

Inflammatory Pathways Are Shut-Down in Infection-Derived MDSC Subsets

Since gene profiling can inform on MDSC features and has been associated with MDSC function (55, 56), we assessed the regulation of innate and adaptive genes comparing isolated Mo-MDSCs and PMN-MDSCs from the TC of infected WT BALB/c mice on day 72 p.i. to those of naive mice which served as controls. Interestingly, data from the PCR array (84 genes) showed that PMN-MDSCs and especially Mo-MDSCs isolated from infected mice displayed an up-regulation of FOXP3 (Forkhead box P3), a transcription factor for regulatory T cells (Tregs) and NF-κB1 (Nuclear factor of kappa light polypeptide gene enhancer in B-cells 1, p105) (**Tables 1**, **2**). However, a down-regulation of genes including C3 (Complement component 3), CCR6 (Chemokine
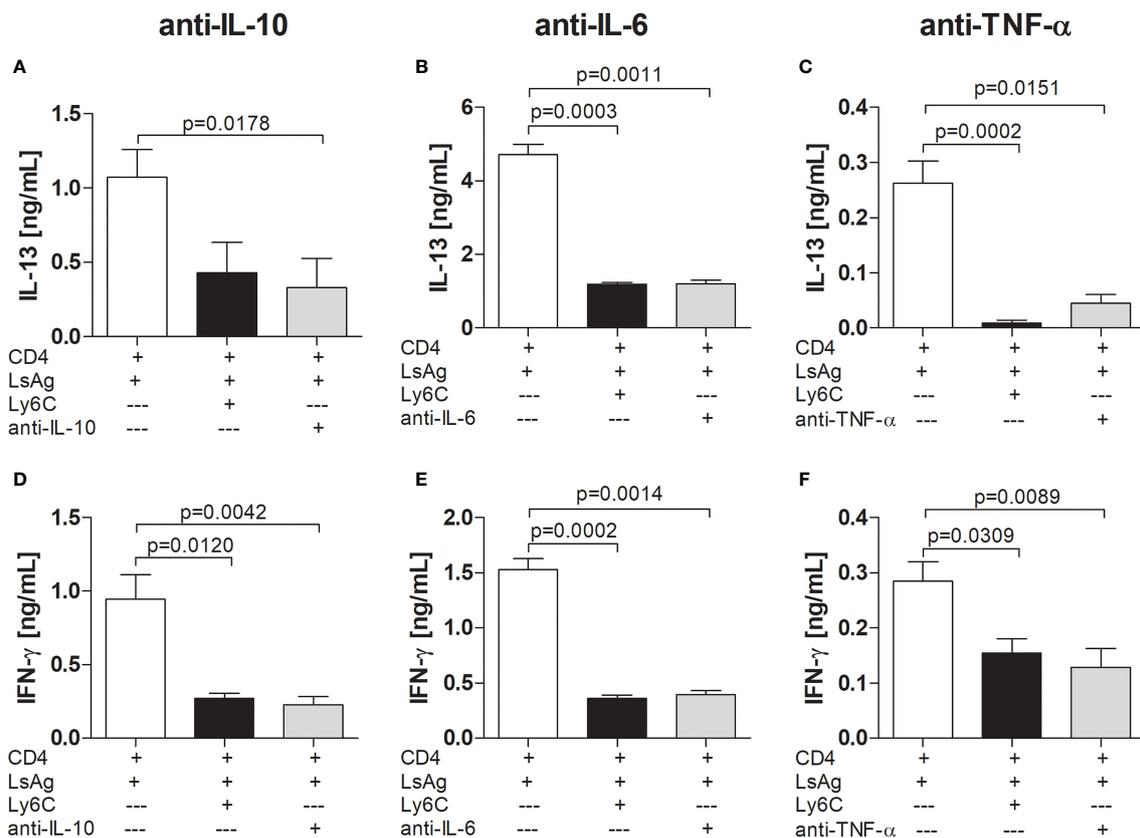
FIGURE 4 | Mo-MDSCs do not require IL-10, IL-6 or TNF-α to suppress filarial-specific CD4+ T cell responses. Day 72 p.i.-derived CD4+ T (1x10^5) cells from Ls-infected BALB/c mice were cultured with GM-CSF-derived BMDCs (5x10^4) and LsAg (50 μg/mL) in the presence or absence of isolated Mo-MDSCs (1x10^5) and with or without anti-IL-10 (2 μg/mL) **(A, D)**, anti-IL-6 (10 μg/mL) **(B, E)** or anti-TNF-α (0.5 μg/mL) **(C, F)** for 72 hours. Supernatants were then screened for IL-13 **(A-C)** and IFN-γ **(D-F)** by ELISA. Each graph shows mean ± SEM of combined co-culture assays using cells from 5-10 pooled mice from two independent infections. Statistical significances between the indicated groups were either obtained after Kruskal-Wallis followed by Dunn's multiple comparison test **(A–E)** or after ANOVA followed by Tukey multiple comparison test **(F)**.

(C-C motif) receptor 6) and IL-18 (Interleukin 18) was observed in the two subsets (**Tables 3, 4**). Mo-MDSCs alone showed negative fold-changes in the expression of the genes IL-1α and NOD1 (Nucleotide-binding oligomerization domain containing 1) (**Table 3**) but displayed up-regulated expression of IFN-γ and IL-13 when compared to those from naive controls (**Table 1**). These results give a primary indication that gene expression within the two MDSC subsets present high regulatory and rather low inflammatory properties.

DISCUSSION

In this study, we show that MDSCs are induced and expanded at the site of infection following exposure to *L. sigmodontis* (**Figure 1**) and moreover that the monocytic subset displays distinct suppressive activities on filarial-specific CD4+ T cell responses (**Figure 2**). Furthermore, the suppression was tailored since not all cytokine responses were suppressed e.g. IL-5 (**Figure 2B**), adding credence to the overall findings.

In cancer, MDSC frequencies have been associated with both the state and progression of pathology (46, 57). Using the laboratory BALB/c mouse strain, which allows the complete Ls life-cycle, we found that in the absence of infection, very few Mo-MDSCs and PMN-MDSCs were within the TC fluid whereas large numbers of these cells were identified after infection (**Figure 1B**). This supports earlier studies that revealed that levels of MDSC populations increase under inflammatory conditions (20, 58). Interestingly, there was a higher number of PMN-MDSCs when compared to Mo-MDSCs (**Figure 1C**) which reflects observations in tumour models (19) but different compositions were found in *Trypanosoma congolense*-infected mice (59). In our model, MDSC infiltration positively correlated with adult worm burden (**Figure 1D**). Therefore, we suggest that while adult worms develop, the host offers a favourable milieu for MDSC infiltration or vice versa, promoting chronic infection. This is in line with recent findings that demonstrated that after adoptive transfer of MDSCs, there was a persistent chronic phase of infection with the nematode *Heligmosomoides polygyrus bakeri* (28).
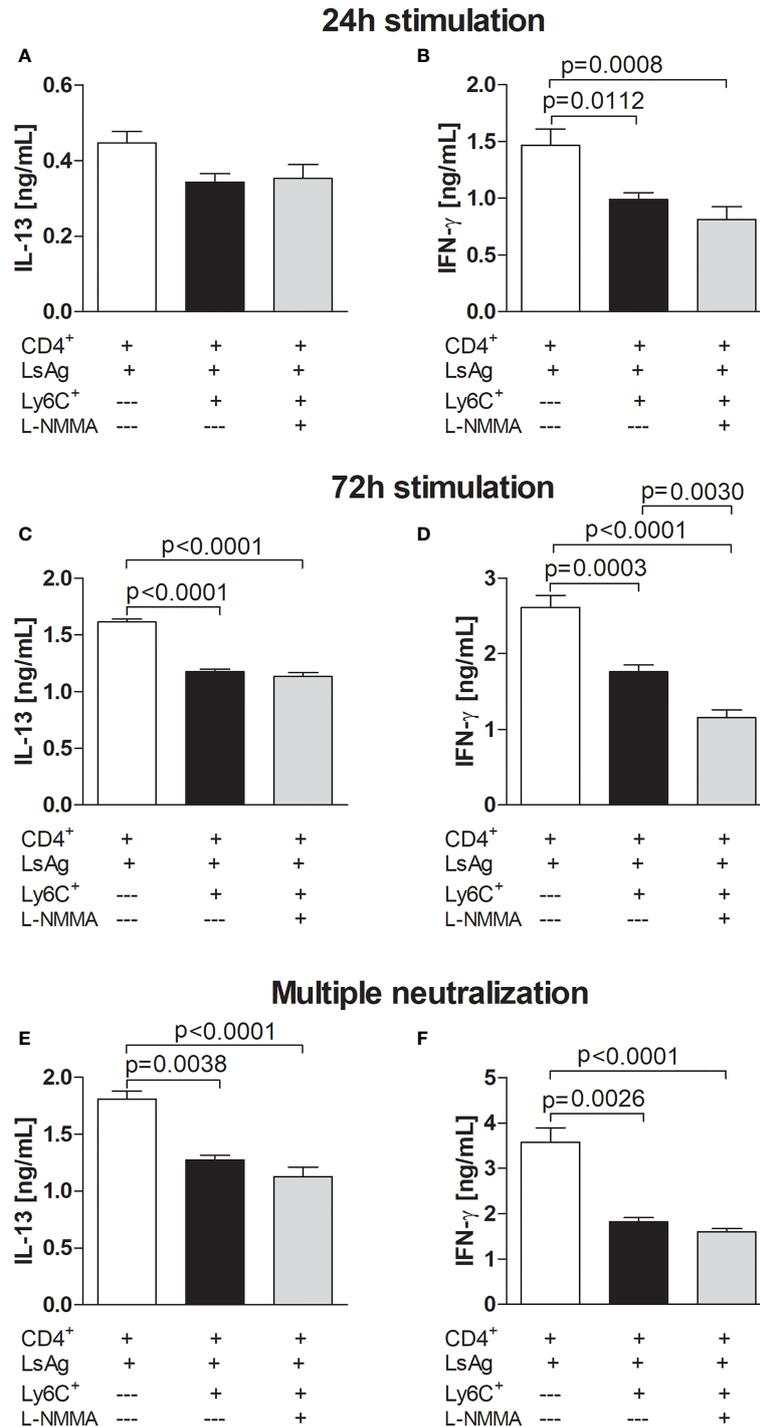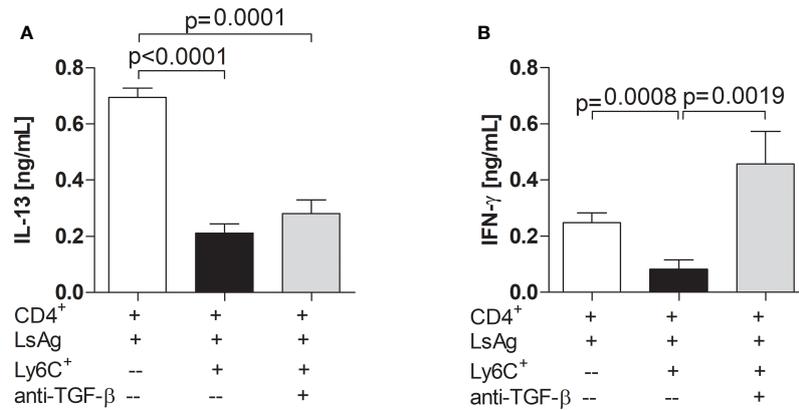
FIGURE 5 | Filarial-derived Mo-MDSCs do not suppress CD4^{+} T cell responses *via* NO pathways. Day 72 p.i.-derived CD4^{+} T (1x10^{5}) cells from Ls-infected BALB/c mice were cultured with GM-CSF-derived BMDCs (5x10^{4}) and LsAg (50 μg/mL) in the presence or absence of isolated Mo-MDSCs (5x10^{4}) and with or without L-NMMA (5 μM). In **(A–D)**, L-NMMA was added at 0 hours whereas in **(E, F)** the inhibitor was added at 0, 24 and 48 hours - multiple neutralization. Supernatants were then screened for IL-13 **(A, C, E)** and IFN-γ **(B, D, F)** by ELISA after 24 hours **(A, B)** or 72 hours **(C-F)**. Graphs **(A, B, E, F)** show mean ± SEM of two co-culture assays using isolated MDSCs from 10 pooled mice. Graphs **C** and **D** show mean ± SEM of one co-culture assay using isolated MDSCs from 10 pooled mice. Statistical significances between the indicated groups were obtained after ANOVA **(B–D)** or Kruskal-Wallis followed by Dunn's multiple comparison test **(E, F)**.

FIGURE 6 | Neutralizing TGF-β abrogates the suppression of IFN-γ production. Day 72 p.i.-derived CD4+ T (1x10^5) cells from Ls-infected BALB/c mice were cultured with GM-CSF-derived BMDCs (5x10^4) and LsAg (50 μg/mL) in the presence or absence of isolated Mo-MDSCs (1x10^5) and with or without anti-TGF-β (10 μg/mL) for 72 hours. Supernatants were then screened for IL-13 **(A)** and IFN-γ **(B)** by ELISA. Each graph shows mean ± SEM of combined co-culture assays using cells from 5-10 pooled mice from three independent infections. Statistical significances between the indicated groups were obtained after Kruskal-Wallis followed by Dunn's multiple comparison test.

Upon re-stimulation of CD4+ T cells from infected mice with LsAg, infection-derived Mo-MDSCs but not PMN-MDSCs were able to impair the release of IFN-γ, and IL-13 but not IL-5 (**Figure 2B**). This suppression was revealed not to be dependent on patency since Mo-MDSCs derived from both MF- and MF+ Ls-infected mice groups were similarly capable of suppression (**Figure S4**). Studies in cancer patients have demonstrated the suppressive function of MDSCs on CD4+ T cell responses even though the effect of Mo-MDSCs was not specifically ascertained (60). In contrast, data from primary glioblastoma patients have indicated that Mo-MDSCs were not able to suppress T cell responses, confining the suppressive function in that scenario to PMN-MDSCs. Indeed, these authors have observed diverse MDSC subsets including monocytic, granulocytic, neutrophilic,

eosinophilic and immature MDSCs (61). In regards to murine settings, Zhu and colleagues found that in a murine model of hepatitis, SSC^{high}CD11b^{high}Ly-6C^{high}Ly-6G^{low}MDSCs, corresponding to Mo-MDSCs, were the only subset capable of suppressing CD4+ T cell responses while the other MDSC-like compartment was not capable of doing so (62). Elsewhere, studies in C57BL/6 mice have noted the inhibition of not only T cell responses but also of B cell responses by Mo-MDSCs in murine LP-BM5 retroviral infections (63, 64). PMN-MDSC numbers in the TC were higher when compared to Mo-MDSCs (**Figure 1C**) but only Mo-MDSCs displayed a suppressive function on LsAg specific CD4+ T cell responses (**Figure 2B**), suggesting that the Mo-MDSC-mediated suppressive function was not associated with elevated Mo-
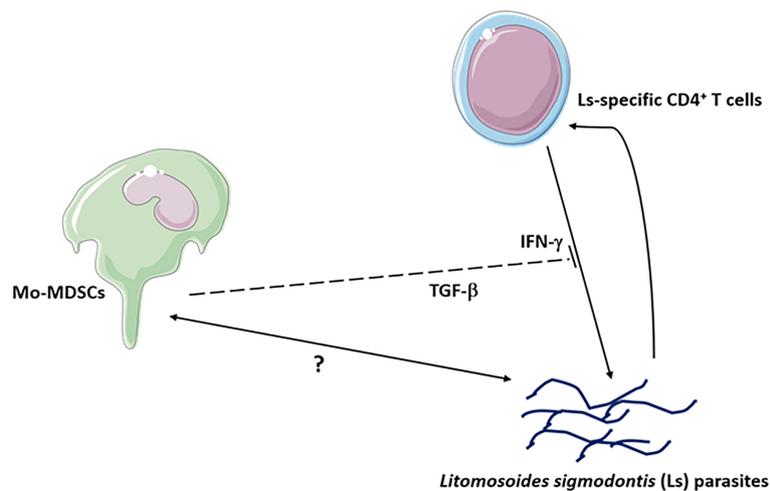

FIGURE 7 | Mo-MDSCs suppress the production of IL-13 and IFN-γ *via* Ls-specific CD4+ T cells. The Mo-MDSC suppressive function of IFN-γ occurs through TGF-β.

TABLE 1 | Up-regulated genes in Ls-infected Mo-MDSCs compared to naïve Mo-MDSCs.

Gene	Full name	Fold change	p-value
Cxcr3	Chemokine (C-X-C motif) receptor 3	1002.9264	0.005499
Fasl	Fas ligand (TNF superfamily, member 6)	5454.886	0.000814
Foxp3	Forkhead box P3	185.2505	0.00323
Ifng	Interferon gamma	15789.3774	0.002364
Il13	Interleukin 13	2923.201	0.027058
Ly96	Lymphocyte antigen 96	10.6295	0.03942
Mpo	Myeloperoxidase	263.1971	0.017737
Myd88	Myeloid differentiation primary response gene 88	3.0035	0.005016
Nfkb1	Nuclear factor of kappa light polypeptide gene enhancer in B-cells 1, p105	3.8548	0.045602
Tbx21	T-box 21	645.0796	0.012174
Tlr8	Toll-like receptor 8	13155.0885	0.015218

MDSC numbers at the site of infection. Given the fact that Mo-MDSCs had a purity rate of 94% after re-analysis (**Figure S1A**), it could be that non Mo-MDSC cells might have contributed to in vitro suppression as well. Although PMN-MDSCs did not suppress filarial-specific $CD4^+$ T cell responses, this does not rule out that these cells have a suppressive capacity in another setting. Moreover, in order to confirm these results, a more sophisticated intracellular FACS staining of the co-cultured cells should be performed in further studies in order to assess clearly the source of the cytokines. To gain further insight into the interaction of these three immune cell types (T cells:Mo-MDSCs : APC) both in vitro and in vivo, future studies should include immune phenotyping of the T cells and APC. A further future line of investigation in this suppressive scenario would be to study the interaction or direct effect of Mo-MDSCs on the APC in the in vitro assay (BM-DC). Since the results from the transwell assays showed that suppression by Mo-MDSCs on the cytokine release from $CD4^+$ T cells was not altered we consider that any effects on the APC by Mo-MDSC would be mediated though soluble factors as well. Although Mo-MDSCs were very scarce in the thoracic cavity, the site of infection, of uninfected mice, further studies should explore the function of Mo-MDSCs from other sites (blood for example) on $CD4^+$ T cells to serve as control and substantiate the specific ability of L. sigmodontis infection-derived Mo-MDSCs to suppress IFN-γ and IL-13 production.

In earlier studies we showed that Ls-infected IL-4Rα/IL-5 dKO BALB/c mice had higher worm burden and full patency when compared to the WT group (9). Since studies have suggested that the presence of the IL-4Rα is associated with the suppressive activity of Mo-MDSCs in melanoma and colon carcinomas (38), we investigated the role of this receptor too.

However, our results clearly show that the lack of IL-4/IL-5 signalling does not impair the suppression of $CD4^+$ T cell responses by Mo-MDSCs (**Figures 3A, B**) but does seem to facilitate Mo-MDSC infiltration into the TC of Ls-infected IL-4Rα/IL-5 dKO BALB/c mice (**Figure S5**). These findings support previous studies which showed that in tumour-harbouring IL-4Rα KO mice, the IL-4Rα receptor was not required for MDSC function (65). Furthermore, our infection-derived Mo-MDSCs kept their suppressive ability even after CCR2 blockade (**Figures 3C, D**). In contrast to that and using MDSCs generated from $CCR2^{-/-}$ C57BL/6 mice, Qin and colleagues showed that these cells failed to migrate to islet allografts and to suppress $CD8^+$ T cells under in vivo conditions which resulted in enhanced Tregs activity. However, they were able to exert in vitro inhibition (66). Further studies are required to ascertain whether blocking CCR2 truly affects the suppressive nature of filarial-specific Mo-MDSCs.

CCR2 is mainly involved in the migration of cells, which occurs during the course of infection. There remains a debate as to whether the anti-CCR2 neutralizing Ab used in this study, was suitable to block the activity of the receptor in vitro although a study reported that anti-CCR2 treatment had minimal influence on tumour regression (67). Perhaps Mo-MDSCs require CCR2 to influence only $CD8^+$ T cell but not $CD4^+$ T cell responses. In addition, the fact that these authors used generated MDSCs could explain the conflicting results observed here. Furthermore, data from Schmid et al. indicated that the CCR2 receptor was impaired in Mo-MDSCs derived from Leishmania major infected BALB/c mice when compared to those from C57BL/6 mice (68), suggesting that the presence and thus the activity of this receptor in mice may be strain-dependent. Therefore, more experiments using $CCR2^{-/-}$ BALB/c mice and especially, using

TABLE 2 | Up-regulated genes in Ls-infected PMN-MDSCs compared to naïve PMN-MDSCs.

Gene	Full name	Fold change	p-value
Cd86	CD86 antigen	63.7049	0.014497
Cxcl10	Chemokine (C-X-C motif) ligand 10	47.9458	0.024228
Foxp3	Forkhead box P3	83.8652	0.003258
Ifnar1	Interferon (alpha and beta) receptor 1	71.8376	0.040521
Nfkb1	Nuclear factor of kappa light polypeptide gene enhancer in B-cells 1, p105	85.8254	0.01314
Nod2	Nucleotide-binding oligomerization domain containing 2	9.2749	0.01544
Stat3	Signal transducer and activator of transcription 3	186.9705	0.009197

TABLE 3 | Down-regulated genes in Ls-infected Mo-MDSCs compared to naïve Mo-MDSCs.

Gene	Full name	Fold change	p-value
C3	Complement component 3	0	0
Ccr5	Chemokine (C-C motif) receptor 5	0	0.015038
Ccr6	Chemokine (C-C motif) receptor 6	0.0302	0.00881
H2-T23	Histocompatibility 2, T region locus 23	0	0.000019
Ifngr1	Interferon gamma receptor 1	0	0.002929
Il18	Interleukin 18	0.0001	0.041412
Il1a	Interleukin 1 alpha	0.1381	0.014621
Irf3	Interferon regulatory factor 3	0	0.000229
Irf7	Interferon regulatory factor 7	0	0.004402
Itgam	Integrin alpha M	0	0.000007
Mapk1	Mitogen-activated protein kinase 1	0	0.000283
Nod1	Nucleotide-binding oligomerization domain containing 1	0.0073	0.045602
Rorc	RAR-related orphan receptor gamma	0.2161	0.00539
Traf6	Tnf receptor-associated factor 6	0	0.000131

MDSCs that lack the CCR2 receptor, are needed to clarify the role that is played within MDSC function. Our data also show that blocking TNF-α did not impair Mo-MDSC function either. These findings contrast with the observations reported by Atretkhany and colleagues who used TNF humanized (hTNF) knock-in mice, to show that blockade of TNF activity ameliorated fibroblastic sarcoma growth and led to a decreased MDSC accumulation (69). Although the findings generated in this study do not indicate a role of apoptosis, for example the lack of effect on IL-5 release, further studies would be needed to substantiate that parameter. Likewise, it would be interesting to decipher the effect of Mo-MDSCs on T cell proliferation in Ls infection setting.

To gain further insight into the Mo-MDSC profiles, we additionally performed a PCR-array on isolated subsets and elucidated several genes that were up- and down-regulated when compared to naïve MDSC populations. These included the gene responsible for IL-1α expression which was shut down in Mo-MDSCs during Ls infection (**Table 3**). Interestingly, MDSCs have been shown to phagocytose *Mycobacterium tuberculosis* and produce high levels of IL-1α (70). Additionally, IL-18, a cytokine released upon activation of the inflammasomes, was found to be down-regulated in both Mo-MDSC and PMN-MDSC subsets isolated from Ls-infected mice, when compared to those of naive mice (**Tables 3**, **4**). The expression of NLRP3 (NOD-like receptor family, pyrin domain containing 3) inflammasome was also down-regulated in PMN-MDSCs (**Tables 4**). Interestingly, studies in patients with cryopyrin-associated periodic syndromes under anti-IL-1 therapy have displayed elevated MDSC numbers with suppressive activity (71). Recent data have indicated a positive

correlation between the NLRP3 inflammasome expression and the MDSC markers CD11b and CD33 in a human head and neck squamous cell carcinoma (HNSCC) tissue microarray (72). Whether the inflammasome-signalling pathway plays a role in the suppressive capacity of filarial-induced Mo-MDSCs requires further studies. Interestingly, preliminary *in vivo* data from Ls-infected ASC$^{-/-}$ BALB/c mice showed no differences in Mo-MDSC numbers on day 72 post-infection (data not shown).

With regards to gene expression profiling, the data-sets here revealed that there was a down-regulation of the complement component C3 gene in both Ls-infected Mo-MDSC and PMN-MDSC subsets. Consistent with these results, an earlier report indicated that a complement component C3 deficiency in a diabetes model, was associated with favourable conditions for MDSC induction and associated disease outcome (73). In contrast, hepatic stellate cells derived from mice lacking complement component C3, have been shown to display an impaired MDSC induction and in doing so, exhibited no protection on co-transplanted islet allografts (74). This indicates that the regulation of the complement component C3 by MDSCs is linked to inflammation scenarios. We found that the FOXP3 gene is up-regulated in Mo-MDSCs and PMN-MDSCs during Ls infection, suggesting that both subsets might share the expression of the transcription factor Foxp3 together with Tregs, which could support their role as regulator of immune responses. Further studies should confirm these data and investigate the role of FOXP3 in MDSCs and how this marker could possibly influence MDSC function.

In summary, our study shows that MDSC subsets accumulate during chronic Ls infection at the site of infection. Moreover,

TABLE 4 | Down-regulated genes in Ls-infected PMN-MDSCs compared to naïve PMN-MDSCs.

Gene	Full name	Fold change	p-value
C3	Complement component 3	0	0
Ccr6	Chemokine (C-C motif) receptor 6	0.0274	0.022937
Il18	Interleukin 18	0.0808	0.020914
Nfkbia	Nuclear factor of kappa light polypeptide gene enhancer in B-cells inhibitor, alpha	0	0
Nlrp3	NLR family, pyrin domain containing 3	0.2295	0.006923

infection-derived Mo-MDSCs exhibit a suppressive function on the production of IL-13 and IFN-γ by Ls-specific CD4$^+$ T cell responses. Strikingly, IFN-γ production was rescued after blocking TGF-β and reveals that Mo-MDSCs are a relevant cell-type involved in filarial immunomodulation. Future studies should incorporate *in vivo* experiments which block Mo-MDSC development during infection or analyze the outcome of infection in the absence of TGF-β. Both scenarios hold difficulties since the long-term administration of neutralizing antibodies could not only alter the outcome of infection *per se* but also the development of host:helminth interactions which could lead to skewed helminth-specific immune responses. Thus, to evaluate the functional role of these subsets *in vivo*, preclinical models need to be established which allow tracking and depletion on-demand capabilities such as the DEREG model (75, 76).

DATA AVAILABILITY STATEMENT

We have provided an additional file in which all raw data related to gene expression findings (PCR array results) are made available.

ETHICS STATEMENT

The animal study was reviewed and approved by Landesamt für Natur, Umwelt und Verbraucherschutz, NRW, Germany.

AUTHOR CONTRIBUTIONS

RSET and LEL designed the research project. RSET, MR, AW, KA and LEL planned and executed experiments. RSET and LEL analysed the data which was then discussed with MR and KA. MM provided the CCR2 blocking antibody. RSET and LEL wrote the manuscript which was then amended and critically assessed by all authors including AH.

SUPPLEMENTARY MATERIAL

The Supplementary Material for this article can be found online at: https://www.frontiersin.org/articles/10.3389/fitd.2021.707100/full#supplementary-material

REFERENCES

1. GBD-2017-Disease-and-Injury-Incidence-and-Prevalence-Collaborators. Global, Regional, and National Incidence, Prevalence, and Years Lived With Disability for 354 Diseases and Injuries for 195 Countries and Territories, 1990-2017: A Systematic Analysis for the Global Burden of Disease Study 2017. *Lancet* (2018) 392(10159):1789–858.
2. Ramaiah KD, Ottesen EA. Progress and Impact of 13 Years of the Global Programme to Eliminate Lymphatic Filariasis on Reducing the Burden of Filarial Disease. *PloS Neglected Trop Dis* (2014) 8(11). doi: 10.1371/journal.pntd.0003319
3. WHO. *Weekly Epidemiological Record*. World: World Health Organization. 92. (2017). pp. 589–608.
4. Turner P, Copeman B, Gerisi D, Speare R. A Comparison of the Og4c3 Antigen Capture Elisa, the Knott Test, an Igg4 Assay and Clinical Signs, in the Diagnosis of Bancroftian Filariasis. *Trop Med Parasitol* (1993) 44(1):45–8.
5. Petit G, Diagne M, Marechal P, Owen D, Taylor D, Bain O, et al. Maturation of the Filaria Litomosoides-Sigmodontis in Balb/C Mice - Comparative

Susceptibility of 9 Other Inbred Strains. *Annales Parasitol Humaine Et Comparee* (1992) 67(5):144–50. doi: 10.1051/parasite/1992675144
6. Rodrigo MB, Schulz S, Krupp V, Ritter M, Wiszniewsky K, Arndts K, et al. Patency of Litomosoides Sigmodontis Infection Depends on Toll-Like Receptor 4 Whereas Toll-Like Receptor 2 Signalling Influences Filarial-Specific CD4(+) T-Cell Responses. *Immunology* (2016) 147(4):429–42. doi: 10.1111/imm.12573
7. Al-Qaoud KM, Taubert A, Zahner H, Fleischer B, Hoerauf A. Infection of BALB/C Mice With the Filarial Nematode Litomosoides Sigmodontis: Role of CD4(+) T Cells in Controlling Larval Development. *Infect Immun* (1997) 65(6):2457–61. doi: 10.1128/iai.65.6.2457-2461.1997
8. Layland LE, Ajendra J, Ritter M, Wiszniewsky A, Hoerauf A, Hubner MP, et al. Development of Patent Litomosoides Sigmodontis Infections in Semi-Susceptible C57BL/6 Mice in the Absence of Adaptive Immune Responses. *Parasites Vectors* (2015) 8. doi: 10.1186/s13071-015-1011-2
9. Ritter M, Tamadaho RSE, Feid J, Vogel W, Wiszniewsky K, Perner S, et al. IL-4/5 Signalling Plays an Important Role During Litomosoides Sigmodontis Infection, Influencing Both Immune System Regulation and Tissue Pathology

in the Thoracic Cavity. *Int J Parasitol* (2017) 47(14):951–60. doi: 10.1016/j.ijpara.2017.06.009

10. Volkmann L, Bain O, Saeftel M, Specht S, Fischer K, Brombacher F, et al. Murine Filariasis: Interleukin 4 and Interleukin 5 Lead to Containment of Different Worm Developmental Stages. *Med Microbiol Immunol* (2003) 192 (1):23–31. doi: 10.1007/s00430-002-0155-9

11. Frohberger SJ, Ajendra J, Surendar J, Stamminger W, Ehrens A, Buerfent BC, et al. Susceptibility to L. Sigmodontis Infection is Highest in Animals Lacking IL-4r/IL-5 Compared to Single Knockouts of IL-4r, IL-5 or Eosinophils. *Parasit Vectors* (2019) 12(1):248. doi: 10.1186/s13071-019-3502-z

12. Saeftel M, Volkmann L, Korten S, Brattig N, Al-Qaoud K, Fleischer B, et al. Lack of Interferon-Gamma Confers Impaired Neutrophil Granulocyte Function and Imparts Prolonged Survival of Adult Filarial Worms in Murine Filariasis. *Microbes Infect* (2001) 3(3):203–13. doi: 10.1016/S1286-4579(01)01372-7

13. Saeftel M, Arndt M, Specht S, Volkmann L, Hoerauf A. Synergism of Gamma Interferon and Interleukin-5 in the Control of Murine Filariasis. *Infect Immun* (2003) 71(12):6978–85. doi: 10.1128/IAI.71.12.6978-6985.2003

14. Jenkins SJ, Allen JE. Similarity and Diversity in Macrophage Activation by Nematodes, Trematodes, and Cestodes. *J Biomed Biotechnol* (2010). doi: 10.1155/2010/262609

15. Taylor MD, Harris A, Babayan SA, Bain O, Culshaw A, Allen JE, et al. CTLA-4 and CD4(+)CD25(+) Regulatory T Cells Inhibit Protective Immunity to Filarial Parasites In Vivo. *J Immunol* (2007) 179(7):4626–34. doi: 10.4049/jimmunol.179.7.4626

16. Taylor MD, Harris A, Nair MG, Maizels RM, Allen JE. F4/80(+) Alternatively Activated Macrophages Control CD4(+) T Cell Hyporesponsiveness at Sites Peripheral to Filarial Infection. *J Immunol* (2006) 176(11):6918–27. doi: 10.4049/jimmunol.176.11.6918

17. Taylor MD, van der Werf N, Harris A, Graham AL, Bain O, Allen JE, et al. Early Recruitment of Natural CD4+ Foxp3+ Treg Cells by Infective Larvae Determines the Outcome of Filarial Infection. *Eur J Immunol* (2009) 39 (1):192–206. doi: 10.1002/eji.200838727

18. Ostrand-Rosenberg S, Sinha P. Myeloid-Derived Suppressor Cells: Linking Inflammation and Cancer. *J Immunol* (2009) 182(8):4499–506. doi: 10.4049/jimmunol.0802740

19. Youn JI, Nagaraj S, Collazo M, Gabrilovich DI. Subsets of Myeloid-Derived Suppressor Cells in Tumor-Bearing Mice. *J Immunol* (2008) 181(8):5791–802. doi: 10.4049/jimmunol.181.8.5791

20. Tamadaho RSE, Hoerauf A, Layland LE. Immunomodulatory Effects of Myeloid-Derived Suppressor Cells in Diseases: Role in Cancer and Infections. *Immunobiology* (2018) 223(4-5):432–42. doi: 10.1016/j.imbio.2017.07.001

21. Xu JJ, Peng YH, Yang MY, Guo NN, Liu HT, Gao H, et al. Increased Levels of Myeloid-Derived Suppressor Cells in Esophageal Cancer Patients Is Associated With the Complication of Sepsis. *Biomed Pharmacother* (2020) 125. doi: 10.1016/j.biopha.2020.109864

22. Brodaczewska KK, Donskow-Lysoniewska K, Krawczak K, Doligalska M. Role of L-Arginine and CD11b+Gr-1+Cells in Immunosuppression Induced by Heligmosomoides Polygyrus Bakeri. *Parasite Immunol* (2020) 42:e12704. doi: 10.1111/pim.12704

23. Guo PL, Li LH, Li WL, Zhao JC, Hu FY, Zhang FC, et al. The Clinical Significance of Myeloid-Derived Suppressor Cells in Dengue Fever Patients. *BMC Infect Dis* (2019) 19(1):926. doi: 10.1186/s12879-019-4574-2

24. Hetta HF, Zahran AM, Mansor SG, Abdel-Malek MO, Mekky MA, Abbas WA, et al. Frequency and Implications of Myeloid-Derived Suppressor Cells and Lymphocyte Subsets in Egyptian Patients With Hepatitis C Virus-Related Hepatocellular Carcinoma. *J Med Virol* (2019) 91(7):1319–28. doi: 10.1002/jmv.25428

25. Zhang XF, Gong WC, Cao SK, Xu M, Cao JP, Shen YJ, et al. [Dynamic Changes of Myeloid-Derived Suppressor Cells and Regulatory T Cells in Livers of Mice Infected With Echinococcus Granulosus]. *Zhongguo Xue Xi Chong Bing Fang Zhi Za Zhi* (2019) 31(6):622–7. doi: 10.16250/j.32.1374.2019154

26. Falck-Jones S, Vangeti S, Yu M, Falck-Jones R, Cagigi A, Badolati I, et al. Functional Monocytic Myeloid-Derived Suppressor Cells Increase in Blood But Not Airways and Predict COVID-19 Severity. *J Clin Invest* (2021). doi: 10.1172/JCI144734

27. Yaseen MM, Abuharfeil NM, Darmani H, Daoud A. Recent Advances in Myeloid-Derived Suppressor Cell Biology. *Front Med* (2020) 15. doi: 10.1007/s11684-020-0797-2

28. Valanparambil RM, Tam M, Jardim A, Geary TG, Stevenson MM. Primary Heligmosomoides Polygyrus Bakeri Infection Induces Myeloid-Derived Suppressor Cells That Suppress CD4(+) Th2 Responses and Promote Chronic Infection. *Mucosal Immunol* (2017) 10(1):238–49. doi: 10.1038/mi.2016.36

29. Ritter M, Krupp V, Wiszniewsky K, Wiszniewsky A, Katawa G, Tamadaho RSE, et al. Absence of IL-17A in Litomosoides Sigmodontis-Infected Mice Influences Worm Development and Drives Elevated Filarial-Specific IFN-Gamma. *Parasitol Res* (2018) 117(8):2665–75. doi: 10.1007/s00436-018-5959-7

30. Hubner MP, Torrero MN, McCall JW, Mitre E. Litomosoides Sigmodontis: A Simple Method to Infect Mice With L3 Larvae Obtained From the Pleural Space of Recently Infected Jirds (Meriones Unguiculatus). *Exp Parasitol* (2009) 123(1):95–8. doi: 10.1016/j.exppara.2009.05.009

31. Layland LE, Mages J, Loddenkemper C, Hoerauf A, Wagner H, Lang R, et al. Pronounced Phenotype in Activated Regulatory T Cells During a Chronic Helminth Infection. *J Immunol* (2010) 184(2):713–24. doi: 10.4049/jimmunol.0901435

32. Layland LE, Rad R, Wagner H, Da Costa CUP. Immunopathology in Schistosomiasis Is Controlled by Antigen-Specific Regulatory T Cells Primed in the Presence of TLR2. *Eur J Immunol* (2007) 37(8):2174–84. doi: 10.1002/eji.200737063

33. Schumak B, Klocke K, Kuepper JM, Biswas A, Djie-Maletz A, Limmer A, et al. Specific Depletion of Ly6C(Hi) Inflammatory Monocytes Prevents Immunopathology in Experimental Cerebral Malaria. *PloS One* (2015) 10 (4). doi: 10.1371/journal.pone.0124080

34. Ballbach M, Dannert A, Singh A, Siegmund DM, Handgretinger R, Piali L, et al. Expression of Checkpoint Molecules on Myeloid-Derived Suppressor Cells. *Immunol Lett* (2017) 192:1–6. doi: 10.1016/j.imlet.2017.10.001

35. Satoguina JS, Adjobimey T, Arndts K, Hoch J, Oldenburg J, Layland LE, et al. Tr1 and Naturally Occurring Regulatory T Cells Induce Igg4 in B Cells Through GITR/GITR-L Interaction, IL-10 and TGF-Beta. *Eur J Immunol* (2008) 38(11):3101–13. doi: 10.1002/eji.200838193

36. Movahedi K, Guilliams M, Van den Bossche J, Van den Bergh R, Gysemans C, Beschin A, et al. Identification of Discrete Tumor-Induced Myeloid-Derived Suppressor Cell Subpopulations With Distinct T Cell-Suppressive Activity. *Blood* (2008) 111(8):4233–44. doi: 10.1182/blood-2007-07-099226

37. Xie ZQ, Ago Y, Okada N, Tachibana M. Valproic Acid Attenuates Immunosuppressive Function of Myeloid-Derived Suppressor Cells. *J Pharmacol Sci* (2018) 137(4):359–65. doi: 10.1016/j.jphs.2018.06.014

38. Mandruzzato S, Solito S, Falisi E, Francescato S, Chiarion-Sileni V, Mocellin S, et al. IL4Ralpha+ Myeloid-Derived Suppressor Cell Expansion in Cancer Patients. *J Immunol* (2009) 182(10):6562–8. doi: 10.4049/jimmunol.0803831

39. Huang B, Lei Z, Zhao J, Gong W, Liu J, Chen Z, et al. CCL2/CCR2 Pathway Mediates Recruitment of Myeloid Suppressor Cells to Cancers. *Cancer Lett* (2007) 252(1):86–92. doi: 10.1016/j.canlet.2006.12.012

40. Gehad AE, Lichtman MK, Schmults CF, Teague JE, Calarese AW, Jiang Y, et al. Nitric Oxide-Producing Myeloid-Derived Suppressor Cells Inhibit Vascular E-Selectin Expression in Human Squamous Cell Carcinomas. *J Invest Dermatol* (2012) 132(11):2642–51. doi: 10.1038/jid.2012.190

41. Lesokhin AM, Hohl TM, Kitano S, Cortez C, Hirschhorn-Cymerman D, Avogadri F, et al. Monocytic CCR2(+) Myeloid-Derived Suppressor Cells Promote Immune Escape by Limiting Activated CD8 T-Cell Infiltration Into the Tumor Microenvironment. *Cancer Res* (2012) 72(4):876–86. doi: 10.1158/0008-5472.CAN-11-1792

42. Flores-Toro JA, Luo D, Gopinath A, Sarkisian MR, Campbell JJ, Charo IF, et al. CCR2 Inhibition Reduces Tumor Myeloid Cells and Unmasks a Checkpoint Inhibitor Effect to Slow Progression of Resistant Murine Gliomas. *Proc Natl Acad Sci USA* (2020) 117(2):1129–38. doi: 10.1073/pnas.1910856117

43. Hu X, Li B, Xiaoyan L, Zhao X, Wan L, Lin G, et al. Transmembrane TNF-A Promotes Suppressive Activities of Myeloid-Derived Suppressor Cells *via* TNFR2. *Jounal Immunol* (2014) 192:1320–31. doi: 10.4049/jimmunol.1203195

44. Sauer H, Wartenberg M, Hescheler J. Reactive Oxygen Species as Intracellular Messengers During Cell Growth and Differentiation. *Cell Physiol Biochem* (2001) 11(4):173–86. doi: 10.1159/000047804

45. Polz J, Remke A, Weber S, Schmidt D, Weber-Steffens D, Pietryga-Krieger A, et al. Myeloid Suppressor Cells Require Membrane TNFR2 Expression for Suppressive Activity. *Immun Inflammation Dis* (2014) 2(2):121–30. doi: 10.1002/iid3.19

46. Arihara F, Mizukoshi E, Kitahara M, Takata Y, Arai K, Yamashita T, et al. Increase in CD14(+)HLA-DR-/Low Myeloid-Derived Suppressor Cells in

Hepatocellular Carcinoma Patients and Its Impact on Prognosis. *Cancer Immunol Immunother* (2013) 62(8):1421–30. doi: 10.1007/s00262-013-1447-1

47. Mao YM, Poschke I, Wennerberg E, de Coana YP, Brage SE, Schultz I, et al. Melanoma-Educated CD14(+) Cells Acquire a Myeloid-Derived Suppressor Cell Phenotype Through COX-2-Dependent Mechanisms. *Cancer Res* (2013) 73(13):3877–87. doi: 10.1158/0008-5472.CAN-12-4115

48. Penaloza HF, Noguera HF, Ahn LP, Vallejos D, Castellanos OP, Vazquez Y, et al. Interleukin-10 Produced by Myeloid-Derived Suppressor Cells Provides Protection to Carbapenem-Resistant Klebsiella Pneumoniae Sequence Type 258 by Enhancing Its Clearance in the Airways. *Infect Immun* (2019) 87(5). doi: 10.1128/IAI.00665-18

49. Jing B, Wang T, Sun B, Xu J, Xu D, Liao Y, et al. IL6/STAT3 Signaling Orchestrates Premetastatic Niche Formation and Immunosuppressive Traits in Lung. *Cancer Res* (2020) 80(4):784–97. doi: 10.1158/0008-5472.CAN-19-2013

50. Ba H, Li B, Li X, Li C, Feng A, Zhu Y, et al. Transmembrane Tumor Necrosis Factor-Alpha Promotes the Recruitment of Mdscs to Tumor Tissue by Upregulating CXCR4 Expression via TNFR2. *Int Immunopharmacol* (2017) 44:143–52. doi: 10.1016/j.intimp.2016.12.028

51. Milette S, Hashimoto M, Perrino S, Qi S, Chen M, Ham B, et al. Sexual Dimorphism and the Role of Estrogen in the Immune Microenvironment of Liver Metastases. *Nat Commun* (2019) 10(1):5745. doi: 10.1038/s41467-019-13571-x

52. Crook KR, Jin M, Weeks M, Rampersad F, Baldi RR, Glekas RM, et al. Myeloid-Derived Suppressor Cells Regulate T Cell and B Cell Responses During Autoimmune Disease. *J Leukoc Biol* (2015) 97(3):573–82. doi: 10.1189/jlb.4A0314-139R

53. Zhang YL, Xu BY, Luan B, Zhang Y, Li YL, Xiong XR, et al. Myeloid-Derived Suppressor Cells (Mdscs) and Mechanistic Target of Rapamycin (Mtor) Signaling Pathway Interact Through Inducible Nitric Oxide Synthase (Inos) and Nitric Oxide (NO) in Asthma. *Am J Trans Res* (2019) 11(9):6170–84.

54. Morikawa M, Derynck R, Miyazono K. TGF-Beta and the TGF-Beta Family: Context-Dependent Roles in Cell and Tissue Physiology. *Cold Spring Harb Perspect Biol* (2016) 8(5). doi: 10.1101/cshperspect.a021873

55. Bronte V, Brandau S, Chen SH, Colombo MP, Frey AB, Greten TF, et al. Recommendations for Myeloid-Derived Suppressor Cell Nomenclature and Characterization Standards. *Nat Commun* (2016) 7:12150. doi: 10.1038/ncomms12150

56. Nachmany I, Bogoch Y, Friedlander-Malik G, Amar O, Bondar E, Zohar N, et al. The Transcriptional Profile of Circulating Myeloid Derived Suppressor Cells Correlates With Tumor Development and Progression in Mouse. *Genes Immun* (2019) 20(7):589–98. doi: 10.1038/s41435-019-0062-3

57. Almand B, Resser JR, Lindman B, Nadaf S, Clark JI, Kwon ED, et al. Clinical Significance of Defective Dendritic Cell Differentiation in Cancer. *Clin Cancer Res* (2000) 6(5):1755–66.

58. Gabrilovich DI, Nagaraj S. Myeloid-Derived Suppressor Cells as Regulators of the Immune System. *Nat Rev Immunol* (2009) 9(3):162–74. doi: 10.1038/nri2506

59. Onyilagha C, Kuriakose S, Ikeogu N, Jia P, Uzonna J. Myeloid-Derived Suppressor Cells Contribute to Susceptibility to Trypanosoma Congolense Infection by Suppressing CD4(+) T Cell Proliferation and IFN-Gamma Production. *J Immunol* (2018) 201(2):507–15. doi: 10.4049/jimmunol.1800180

60. Ren JP, Zhao J, Dai J, Griffin JWD, Wang L, Wu XY, et al. Hepatitis C Virus-Induced Myeloid-Derived Suppressor Cells Regulate T-Cell Differentiation and Function *via* the Signal Transducer and Activator of Transcription 3 Pathway. *Immunology* (2016) 148(4):377–86. doi: 10.1111/imm.12616

61. Dubinski D, Wolfer J, Hasselblatt M, Schneider-Hohendorf T, Bogdahn U, Stummer W, et al. CD4(+) T Effector Memory Cell Dysfunction Is Associated With the Accumulation of Granulocytic Myeloid-Derived Suppressor Cells in Glioblastoma Patients. *Neuro-Oncology* (2016) 18(6):807–18. doi: 10.1093/neuonc/nov280

62. Zhu K, Zhang N, Guo N, Yang J, Wang J, Yang C, et al. SSC(High)CD11b (High)Ly-6c(High)Ly-6g(Low) Myeloid Cells Curtail CD4 T Cell Response by Inducible Nitric Oxide Synthase in Murine Hepatitis. *Int J Biochem Cell Biol* (2014) 54:89–97. doi: 10.1016/j.biocel.2014.07.005

63. Green KA, Cook WJ, Green WR. Myeloid-Derived Suppressor Cells in Murine Retrovirus-Induced AIDS Inhibit T- and B-Cell Responses *In Vitro* That are Used to Define the Immunodeficiency. *J Virol* (2013) 87(4):2058–71. doi: 10.1128/JVI.01547-12

64. Rastad JL, Green WR. Myeloid-Derived Suppressor Cells in Murine AIDS Inhibit B-Cell Responses in Part *via* Soluble Mediators Including Reactive Oxygen and Nitrogen Species, and TGF-Beta. *Virology* (2016) 499:9–22. doi: 10.1016/j.virol.2016.08.031

65. Sinha P, Parker KH, Horn L, Ostrand-Rosenberg S. Tumor-Induced Myeloid-Derived Suppressor Cell Function Is Independent of IFN-Gamma and IL-4r Alpha. *Eur J Immunol* (2012) 42(8):2052–9. doi: 10.1002/eji.201142230

66. Qin J, Arakawa Y, Morita M, Fung JJ, Qian S, Lu L, et al. C-C Chemokine Receptor Type 2 (CCR2)-Dependent Migration of Myeloid-Derived Suppressor Cells in Protection of Islet Transplants. *Transplantation* (2016). doi: 10.1097/TP.0000000000001529

67. Liang H, Deng L, Hou Y, Meng X, Huang X, Rao E, et al. Host STING-Dependent MDSC Mobilization Drives Extrinsic Radiation Resistance. *Nat Commun* (2017) 8(1):1736. doi: 10.1038/s41467-017-01566-5

68. Schmid M, Zimara N, Wege AK, Ritter U. Myeloid-Derived Suppressor Cell Functionality and Interaction With Leishmania Major Parasites Differ in C57BL/6 and BALB/C Mice. *Eur J Immunol* (2014) 44(11):3295–306. doi: 10.1002/eji.201344335

69. Atretkhany KS, Nosenko MA, Gogoleva VS, Zvartsev RV, Qin Z, Nedospasov SA, et al. TNF Neutralization Results in the Delay of Transplantable Tumor Growth and Reduced MDSC Accumulation. *Front Immunol* (2016) 7:147. doi: 10.3389/fimmu.2016.00147

70. Knaul JK, Jorg S, Oberbeck-Mueller D, Heinemann E, Scheuermann L, Brinkmann V, et al. Lung-Residing Myeloid-Derived Suppressors Display Dual Functionality in Murine Pulmonary Tuberculosis. *Am J Respir Crit Care Med* (2014) 190(9):1053–66. doi: 10.1164/rccm.201405-0828OC

71. Ballbach M, Hall T, Brand A, Neri D, Singh A, Schaefer I, et al. Induction of Myeloid-Derived Suppressor Cells in Cryopyrin-Associated Periodic Syndromes. *J Innate Immun* (2016) 8(5):493–506. doi: 10.1159/000446615

72. Chen L, Huang CF, Li YC, Deng WW, Mao L, Wu L, et al. Blockage of the NLRP3 Inflammasome by MCC950 Improves Anti-Tumor Immune Responses in Head and Neck Squamous Cell Carcinoma. *Cell Mol Life Sci* (2018) 75(11):2045–58. doi: 10.1007/s00018-017-2720-9

73. Gao JJ, Wu YM, Su ZL, Barnie PA, Jiao ZJ, Bie QL, et al. Infiltration of Alternatively Activated Macrophages in Cancer Tissue Is Associated With MDSC and Th2 Polarization in Patients With Esophageal Cancer. *PloS One* (2014) 9(8). doi: 10.1371/journal.pone.0104453

74. Hsieh CC, Chou HS, Yang HR, Lin F, Bhatt S, Qin J, et al. The Role of Complement Component 3 (C3) in Differentiation of Myeloid-Derived Suppressor Cells. *Blood* (2013) 121(10):1760–8. doi: 10.1182/blood-2012-06-440214

75. Layland LE, Straubinger K, Ritter M, Loffredo-Verde E, Garn H, Sparwasser T, et al. Schistosoma Mansoni-Mediated Suppression of Allergic Airway Inflammation Requires Patency and Foxp3(+) Treg Cells. *PloS Neglected Trop Dis* (2013) 7(8). doi: 10.1371/journal.pntd.0002379

76. Lahl K, Loddenkemper C, Drouin C, Freyer J, Arnason J, Eberl G, et al. Selective Depletion of Foxp3(+) Regulatory T Cells Induces a Scurfy-Like Disease. *J Exp Med* (2007) 204(1):57–63. doi: 10.1084/jem.20061852

77. RSE, T. *The Relevance of Myeloid-Derived Suppressor Cells During Litomosoides Sigmodontis Infection. Ph.D. Thesis.* Bonn, Germany: University of Bonn (2018).